*Macromolecules* **1998,** *31,* 8757−8765

# Synthesis and Solution Properties of New Linear-Dendritic Diblock Copolymers

**Jyotsna Iyer, Kala Fleming, and Paula T. Hammond***

*Department of Chemical Engineering, Massachusetts Institute of Technology, Cambridge, Massachusetts 02139*

*Received April 23, 1998; Revised Manuscript Received October 12, 1998*

ABSTRACT: The design and synthesis of new linear-dendritic diblock copolymers with a linear PEO block and a dendrimeric PAMAM block are described. Two series with PEO molecular weights of 2000 and 5000 were synthesized. DSC results on the effect of diblock composition on the microphase segregation behavior of the diblocks are reported. Glass transition temperatures of the diblocks depend on the end group functionality of the dendrimer. The aqueous solution behavior of the hybrid copolymers at 30 °C studied using intrinsic viscosity and GPC techniques is influenced by the length of the PEO block and the end group functionality of the dendrimer. The intrinsic viscosity trends exhibited by the diblocks with the shorter PEO chain length did not deviate greatly from that of linear polymers, and those exhibited by the diblocks with the longer PEO chain length indicate the formation of unimolecular micelles.

## 1.0. Introduction

Dendrimers have been of particular interest to the polymer science community in the past 20 years. These materials present a new, well-defined architecture and a large degree of functionality in a single macromolecule. A wide variety of dendrimers with different chemistries have been synthesized;[1−3] however, commercial applications of these materials have only recently begun to be realized. Many of the potential applications under investigation make use of two important properties of dendrimers, both of which are a direct consequence of their architecture: namely, the large number of end groups and the nanoporous nature of the interior at higher generations.[4] The interior regions may be used to sequester ions, to host molecules, or to act as catalytic sites for reaction of small molecules. When appropriately configured in consistent thin films, dendrimeric materials could prove to be useful as membranes for separations applications. Dendrimeric-linear hybrid diblock copolymers present material systems which are suitable for the formation of self-assembled films in the bulk state, on surfaces, and at the air−water interface. Dendrimeric diblock copolymers with one linear block and one dendritic block have been synthesized by a number of different groups. Examples include PEO−poly(L-lysine) dendrimer,[5] PS−poly(propyleneimine) dendrimer,[6] PEO/PS−poly(benzyl ether) dendrimer,[7,8] and poly(oxazoline)−PAMAM dendrimer.[9] In some cases the aqueous solubility of the two blocks was dissimilar and the resulting diblocks have been shown to be amphiphilic.[5,6,9] We have chosen to investigate an amphiphilic dendrimeric diblock copolymer with a hydrophobic dendron unit and a water soluble linear tail.

Thus far, limited information is available on the dilute solution behavior of dendrimeric diblocks. Deviations from traditional linear behavior of polymers has been observed for dendrimeric homopolymers and block copolymers by other researchers.[1,10] The exponential increase of molecular weight in dendrimeric homopolymers, when compared to a linear incremental increase of molecular diameter with generation, results in large variations from ideal polymer behavior. In the hybrid linear-dendritic diblocks, the additional effect of the linear block can act to modulate or emphasize these deviations, depending on the interactions between the dendrimeric and linear blocks. For example, unimolecular micelles have been reported at low concentrations,[7] and some researchers report the formation of micellar aggregates at critical concentrations.[5,6,9]

Here we report the synthesis of a new series of hybrid linear-dendritic diblock copolymers with poly(ethylene oxide) (PEO) as the linear block and poly(amidoamine) (PAMAM) as the dendritic block. We have designed and synthesized this series of hybrid dendrimer block copolymers specifically for the formation of ultrathin film membranes. To better understand the adsorption behavior and the amphiphilic nature of the synthesized polymers, we also report the effect of PEO chain length and dendrimer end group functionality on the solution behavior of these diblocks. The thermal phase behavior of the bulk diblock copolymers as a function of composition and dendrimer end group functionality are reported, and finally, a study of the glass transition temperatures of these linear-dendrimer hybrid diblock copolymers as a function of end group and block size is also reported. Each of these properties is discussed and compared to the respective property for spherical dendrimers and, where relevant, for linear hybrid systems reported by other groups.

## 2.0. Experimental Section

**2.1. Materials.** Chromatographically pure methoxy−PEO−amine with molecular weights of 2000 and 5000 were purchased from Shearwater Polymers. Methyl acrylate (99+%) purchased from Aldrich was washed two times with equal amounts of 5% NaOH solution followed by MilliQ (18.2 MΩ cm) water to remove the hydroquinone monomethyl ether inhibitor. The washed methyl acrylate was dried over anhydrous magnesium sulfate overnight before use. Ethylenediamine (99+%) bought from Aldrich was distilled before use.

**2.2. Instrumentation.** $^1$H NMR spectra were recorded at room temperature on a Bruker 400 (400 MHz) instrument. FTIR spectra of films cast on KBr pellet were recorded on a Nicolet Magna-IR 550 spectrometer. DSC data were obtained on a Perkin-Elmer DSC7 calorimeter. Heating rates were 10 °C/min. Size exclusion chromatography was performed on a

10.1021/ma980654g CCC: $15.00

Perkin-Elmer system with $NaNO_3$(0.05 M)/$NaN_3$ (0.02%) aqueous solution as the mobile phase at 30 °C. The GPC separation was achieved over three columns (Waters Ultrahydrogel 250, 500, 2000) varying in pore sizes from 250 Å to 2000 Å. PEO standards ranging in molecular weight from 145 000 to 2000 were used for calibration. A Cannon-Ubbelohde semimicro(50) viscometer was used for the intrinsic viscosity measurements. A Bruker BIFLEX III MALDI−TOF MS was used in the reflector mode with a HABA matrix at 20 kV for recording the spectra of PEO(5000)-1.5G and PEO(5000)-2.5G. A Bruker PROFLEX MALDI−TOF MS was used with an αC−I matrix for recording the spectra of PEO(5000)-3.5G and PEO(5000)-4.5G.

**2.3. Synthesis Procedure. PEO(5000) Diblock Series. PEO(5000)-0.5G.** A 2.5 g sample of pure $CH_3O-PEO-NH_2$(5000) was dissolved in 12.5 mL of methanol and added dropwise to 35 mL of purified methyl acrylate kept at 35 °C. After 48 h, the methanol and unreacted methyl acrylate were removed under vacuum, leaving a sticky white residue. The residue was washed with at least 400 mL of ethyl ether to remove any residual impurities and filtered off to give the product, a white solid. The solid product, $CH_3O-PEO-N{<}(CH_2CH_2COOCH_3)_2$ {PEO(5000)-0.5G}, was dried under vacuum. (Yield = 2.34 g, 93%.)

$^1$H NMR in DMSO-$d_6$: $\delta_{PEO}(C\mathbf{H}_2C\mathbf{H}_2O)$ = 3.515 (b); $\delta_{PEO}(C\mathbf{H}_3O-)$ = 3.246 (s); $\delta_{PAMAM}(-COOC\mathbf{H}_3)$ = 3.578 (s); $\delta_{PAMAM}(-C\mathbf{H}_2COOCH_3)$ = 2.399 (t); $\delta_{PAMAM}$(protons next to tertiary amines) = 2.55−2.8 (m). FTIR peaks, $\nu$ cm$^{-1}$: 1113, 1735, 2882.

**PEO(5000)-1.0G.** A 2.24 g sample of PEO(5000)-0.5G was dissolved in 8 mL of methanol and added dropwise to 16.5 mL of freshly distilled ethylenediamine containing 0.0044 g of NaCN. After 48 h at 50 °C, methanol and ethylenediamine were removed under vacuum. The residue obtained was washed with 300−400 mL of ethyl ether and filtered off to give the product. The white solid product, $CH_3O-PEO-N(CH_2CH_2CONHCH_2CH_2NH_2)_2$ {PEO(5000)-1.0G}, was dried under vacuum. (Yield = 2.14 g, 95%.)

$^1$H NMR in DMSO-$d_6$: $\delta_{PEO}(C\mathbf{H_2}C\mathbf{H_2}O)$ = 3.513 (b); $\delta_{PEO}(C\mathbf{H_3}O-)$ = 3.244 (s); $\delta_{PAMAM}(-C\mathbf{H_2}CONH-)$ = 2.19 (m); $\delta_{PAMAM}(-CONHC\mathbf{H_2}-)$ = 3.037 (m); $\delta_{PAMAM}$(protons next to primary and tertiary amines) = 2.5−2.8 (m). FTIR peaks, $\nu$ cm$^{-1}$: 1106, 1541, 1662, 2875, 3270.

**PEO(5000)-1.5G.** A 2.04 g sample of PEO(5000)-1.0G was dissolved in 16.5 mL of methanol and added dropwise to 30 mL of purified methyl acrylate kept at 35 °C. After 42 h, the methanol and unreacted methyl acrylate were removed under vacuum. The white residue was washed with at least 400 mL of ethyl ether and filtered off to give a solid white product, PEO(5000)-1.5G. The solid product was further dried under vacuum. (Yield = 1.906 g, 93%.)

$^1$H NMR in DMSO-$d_6$: $\delta_{PEO}(C\mathbf{H_2}C\mathbf{H_2}O)$ = 3.5 (b); $\delta_{PEO}(C\mathbf{H_3}O-)$ = 3.23 (s); $\delta_{PAMAM}(-COOC\mathbf{H_3})$ = 3.6 (s); $\delta_{PAMAM}(-C\mathbf{H_2}CONH-)$ = 2.16 (m); $\delta_{PAMAM}(-CONHC\mathbf{H_2}-)$ = 3.05 (m); $\delta_{PAMAM}(-C\mathbf{H_2}COOCH_3)$ = 2.4 (m); $\delta_{PAMAM}$(protons next to tertiary amines) = 2.5−2.7 (b). FTIR peaks, $\nu$ cm$^{-1}$: 1115, 1540, 1661, 1734, 2880, 3237.

**PEO(5000)-2.0G.** A 1.75 g sample of PEO(5000)-1.5G was dissolved in 12 mL of methanol and added dropwise to 34 mL of ethylenediamine containing 0.0067 g of NaCN. After 48 h at 50 °C, methanol and ethylenediamine were removed under vacuum. The residue obtained was washed with 300−400 mL of ethyl ether and filtered off to give the product. The product, PEO(5000)-2.0G, was a white solid and was dried over vacuum. (Yield = 1.74 g, 99%.)

$^1$H NMR in DMSO-$d_6$: $\delta_{PEO}(C\mathbf{H_2}C\mathbf{H_2}O)$ = 3.509 (b); $\delta_{PEO}(C\mathbf{H_3}O-)$ = 3.24 (s); $\delta_{PAMAM}(-C\mathbf{H_2}CONH-)$ = 2.191 (m); $\delta_{PAMAM}(-CONHC\mathbf{H_2}-)$ = 3.072 (m); $\delta_{PAMAM}$(protons next to primary and tertiary amines) = 2.5−2.8 (m). FTIR peaks, $\nu$ cm$^{-1}$: 1111, 1549, 1649, 2883, 3277.

**PEO(5000)-2.5G.** A 1.6 g sample of PEO(5000)-2.0G was dissolved in 25 mL of methanol and added dropwise to 22 mL of methyl acrylate. After 24 h, methanol and the unreacted methyl acrylate were removed under vacuum, and the white product washed with about 400 mL of ethyl ether. PEO(5000)-2.5G was filtered off and dried under vacuum. (Yield = 1.43, 89%.)

$^1$H NMR in DMSO-$d_6$: $\delta_{PEO}(C\mathbf{H_2}C\mathbf{H_2}O)$ = 3.51 (b); $\delta_{PEO}(C\mathbf{H_3}O-)$ = 3.247 (s); $\delta_{PAMAM}(-COOC\mathbf{H_3})$ = 3.583 (s); $\delta_{PAMAM}(-C\mathbf{H_2}CONH-)$ = 2.16 (m); $\delta_{PAMAM}(-CONHC\mathbf{H_2}-)$ = 3.06 (m); $\delta_{PAMAM}(-C\mathbf{H_2}COOCH_3)$ = 2.41 (m); $\delta_{PAMAM}$(protons next to tertiary amines) = 2.5−2.7. FTIR peaks, $\nu$ cm$^{-1}$: 1113, 1539, 1662, 1733, 2880, 3258.

**PEO(5000)-3.0G.** A 1.3 g sample of PEO(5000)-2.5G was dissolved in 10 mL of methanol and added dropwise to 20 mL of ethylenediamine. After 55 h at 50 °C, methanol and ethylenediamine were removed under vacuum. The residue was washed with about 400 mL of ethyl ether and the precipitate filtered off to give the solid product, PEO(5000)-3.0G. PEO(5000)-3.0G was dried under vacuum. (Yield = 1.09 g, 83%.)

$^1$H NMR in $D_2O$: $\delta_{PEO}(C\mathbf{H_2}C\mathbf{H_2}O)$ = 3.7 (b); $\delta_{PEO}(C\mathbf{H_3}O-)$ = 3.384 (s); $\delta_{PAMAM}(-C\mathbf{H_2}CONH-)$ = 2.449 (m); $\delta_{PAMAM}(-CONHC\mathbf{H_2}-)$ = 3.31 (m); $\delta_{PAMAM}$(protons next to primary and tertiary amines) = 2.6−2.9. FTIR peaks, $\nu$ cm$^{-1}$: 1111, 1548, 1646, 2878, 3272.

**PEO(5000)-3.5G.** A 0.98 g sample of PEO(5000)-3.0G was dissolved in 15 mL of methanol and added slowly to 13 mL of methyl acrylate. After 24 h, the methanol and methyl acrylate were removed under vacuum. The product, PEO(5000)-3.5G, was washed with at least 200−300 mL of ethyl ether and dried over vacuum. (Yield = 0.97 g, 99%.)

$^1$H NMR in DMSO-$d_6$: $\delta_{PEO}(C\mathbf{H_2}C\mathbf{H_2}O)$ = 3.507 (b); $\delta_{PEO}(C\mathbf{H_3}O-)$ = 3.24 (s); $\delta_{PAMAM}(-COOC\mathbf{H_3})$ = 3.573 (s); $\delta_{PAMAM}(-C\mathbf{H_2}CONH-)$ = 2.175 (m); $\delta_{PAMAM}(-CONHC\mathbf{H_2}-)$ = 3.05 (m); $\delta_{PAMAM}(-C\mathbf{H_2}COOCH_3)$ = 2.407 (m); $\delta_{PAMAM}$(protons next to tertiary amines) = 2.5−2.8. FTIR peaks, $\nu$ cm$^{-1}$: 1112, 1542, 1658, 1733, 2884, 3261.

**PEO(5000)-4.0G.** A 0.809 g sample of PEO(5000)-3.5G was dissolved in 9 mL of methanol and added to 18 mL of ethylenediamine slowly. After 54 h at 50 °C, the methanol and ethylenediamine were removed under vacuum. The residue is washed with 400 mL of ethyl ether, filtered off, and dried over vacuum.

$^1$H NMR in $D_2O$: $\delta_{PEO}(C\mathbf{H_2}C\mathbf{H_2}O)$ = 3.7 (b); $\delta_{PEO}(C\mathbf{H_3}O-)$ = 3.377 (s); $\delta_{PAMAM}(-C\mathbf{H_2}CONH-)$ = 2.43 (m); $\delta_{PAMAM}(-CONHC\mathbf{H_2}-)$ = 3.294 (m); $\delta_{PAMAM}$(protons next to primary and tertiary amines) = 2.5−2.85. FTIR peaks, $\nu$ cm$^{-1}$: 1113, 1549, 1645, 2880, 3273.

**PEO(5000)-4.5G.** A 0.4 g sample of PEO(5000)-4.0G was dissolved in 7.5 mL of methanol and added slowly to 6.5 mL of methyl acrylate. After 24 h, methanol and unreacted methyl acrylate were removed under vacuum. The residue was washed with 400 mL of ethyl ether, filtered off, and dried over vacuum to give the product, PEO(5000)-4.5G.

$^1$H NMR in $CDCl_3$: $\delta_{PEO}(C\mathbf{H_2}C\mathbf{H_2}O)$ = 3.654 (b); $\delta_{PEO}(C\mathbf{H_3}O-)$ = 3.39 (s); $\delta_{PAMAM}(-COOC\mathbf{H_3})$ = 3.677 (s); $\delta_{PAMAM}(-C\mathbf{H_2}CONH-)$ = 2.373 (m); $\delta_{PAMAM}(-CONHC\mathbf{H_2}-)$ = 3.28 (m); $\delta_{PAMAM}(-C\mathbf{H_2}COOCH_3)$ = 2.444 (m); $\delta_{PAMAM}$(protons next to tertiary amines) = 2.5−2.9. FTIR peaks, $\nu$ cm$^{-1}$: 1112, 1541, 1654, 1734, 2887, 3291.

In general, all the synthesis steps described above produced yields of about 80−95%. Higher yields were obtained when care was taken to ensure complete removal of solvent (methanol) and excess reactants (methyl acrylate and ethylenediamine) using vacuum after completion of the reactions. The poor solubility of the PEO linear block in anhydrous ethyl ether was exploited to effectively separate the diblock products and the reactants. NaCN was initially used as a mild catalyst in the amidation step,[11] but subsequent synthesis of the linear-dendrimer diblock series without the NaCN catalyst has shown the catalyst to be unnecessary.

**PEO(2000) Diblock Series.** The synthesis procedure for the PEO(2000)-dendrimer diblock series from PEO(2000) core follows the scheme and molar concentrations outlined above for the PEO(5000)-dendrimer diblock series. The details of the

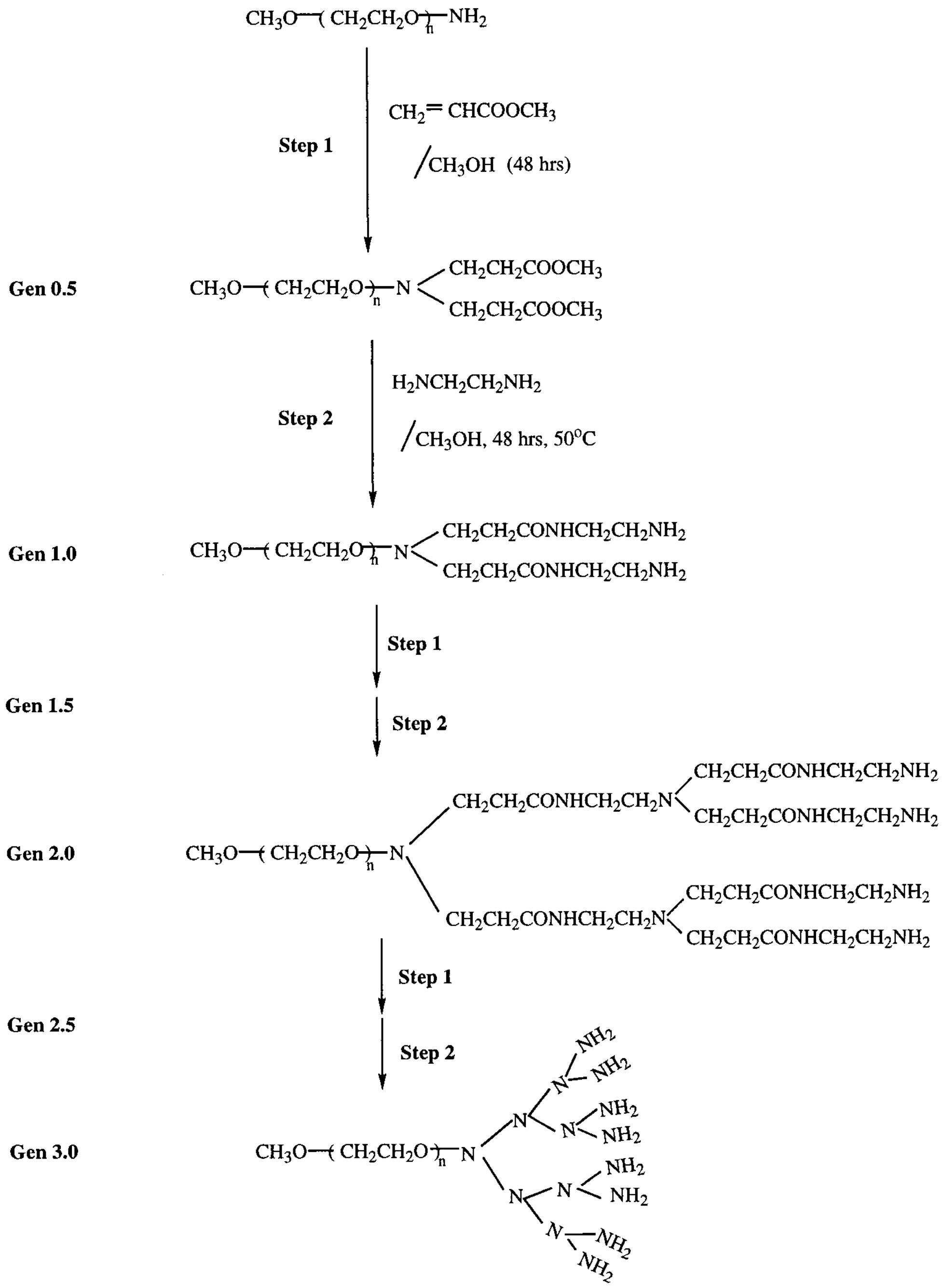

**Figure 1.** Synthesis of PEO–PAMAM diblock copolymer.

NMR and FTIR spectra for the PEO(2000) diblock series synthesized are given in the appendix.

## 3.0. Results and Discussion

**3.1. Design, Synthesis, and Structural Characterization.** A new series of dendrimeric amphiphilic block copolymers were synthesized following the scheme shown in Figure 1. The molecular architecture of these hybrid block copolymers (shown in Figure 2) includes a PAMAM dendron block, chosen for its ease of synthesis and functionalizable terminal amino groups. The linear block of PEO was chosen because PEO is soluble in water and many organic solvents and is available in a number of different molecular weights. These amphiphilic copolymers have been designed to form monolayers at the air–water interface in a Langmuir–Blodgett trough; in these systems, the functionalized hydrophobic dendron is expected to lie at the air side of the interface (Figure 2). Such monolayers can be transferred onto a solid substrate to build multilayer films of the hybrid copolymers with the purpose of forming ultrathin nanoporous films.[12]

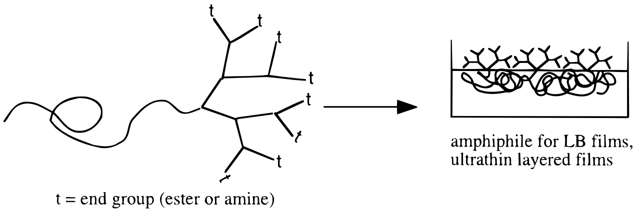

**Figure 2.** Monolayer of dendrimeric block copolymer at the air–water interface.

The synthesis of the PAMAM dendrimer block onto a $CH_3O$–PEO–$NH_2$ core consists of two steps alternately repeated to achieve higher generations and

**Table 1. Theoretically Expected and Experimentally Obtained Ratio between the Unreactive PEO Methoxy Terminal Group and the Methyl Terminal Groups of the Half Generation PEO−PAMAM Diblock Copolymers**

$$\overset{a}{\mathbf{CH_3}}O\text{—}(CH_2CH_2O)_nN<\{[CH_2CH_2COO\overset{b}{\mathbf{CH_3}}]_2\}_m$$

| PEO−PAMAM diblock | no. of dendrimer end groups (theoretical) | a:b theor ratio | a:b exp ratio | $M_w$(theor) | $M_w$(MALDI−TOF) |
|---|---|---|---|---|---|
| PEO(5000)−0.5G | 2 | 3:6 | 3:6 | 5174 | |
| PEO(5000)−1.5G | 4 | 3:12 | 3:13.2 | 5400 | 5960 |
| PEO(5000)−2.5G | 8 | 3:24 | 3:21.4 | 6374 | 6056 |
| PEO(5000)−3.5G | 16 | 3:48 | 3:46.2 | 7974 | 7900 |
| PEO(5000)−4.5G | 32 | 3:96 | 3:92.4 | 11174 | 10750 |
| PEO(2000)−0.5G | 2 | 3:6 | 3:6.3 | 2174 | |
| PEO(2000)−1.5G | 4 | 3:12 | 3:12.8 | 2400 | |
| PEO(2000)−2.5G | 8 | 3:24 | 3:43.5[a] | 3374 | |
| PEO(2000)−3.5G | 16 | 3:48 | 3:50 | 4974 | |

[a] A small amount of the reactant, methyl acrylate {$CH_2{=}CHCOOCH_3$}, was present and contributed to the signal at 3.65 ppm.

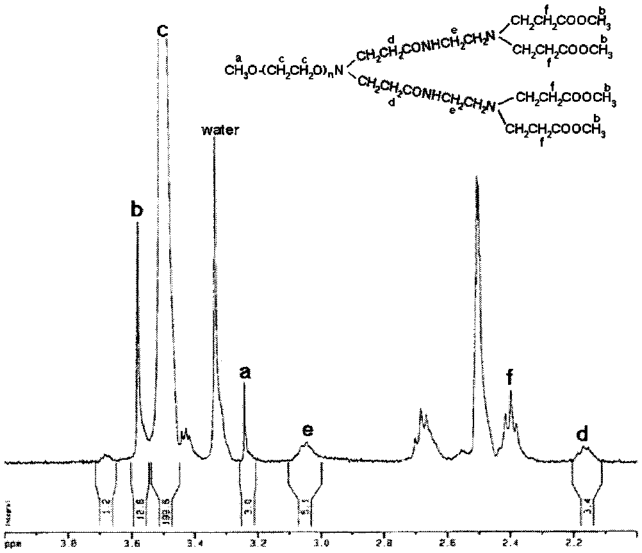

**Figure 3.** $^1H$ NMR spectra of PEO(2000)-1.5G in DMSO-$d_6$.

follows the divergent synthesis technique established by Tomalia.[13] In the first step, exhaustive Michael addition of methyl acrylate to the primary amine terminal groups of the PEO core results in a tertiary amine branch point with methyl ester terminal groups (Figure 1). The methyl ester terminal group is reacted in the second step with ethylenediamine to regenerate the primary amine terminal groups (Step 2). Using this scheme, two series of diblock copolymers with a linear PEO block and a dendritic polyamidoamine block were synthesized. In the first series, the PEO tail had a molecular weight of 2000 with dendrimer generations up to 4.0 [PEO2k-0.5G,1.0G,1.5G,...,4.0G]. In the second series, the PEO tail had a molecular weight of 5000 with dendrimer generations going up to 4.5 [PEO5k-0.5G,1.0G,1.5G,...,4.5G].

Most of the synthesized materials were white partially crystalline solids at room temperature. The chemical structure of the copolymers synthesized was ascertained using $^1H$ NMR and MALDI−TOF as described in detail in the Experimental Section. For illustrative purposes, the $^1H$ NMR spectra of PEO2k-1.5G is shown in Figure 3. The extent of conversion was measured by comparing the integral areas of the dendrimer $^1H$ peaks to that of the unreactive methoxy end group of the PEO tail. A good correspondence was found between the theoretically expected and experimentally obtained values for all the products synthesized, as shown in Table 1. MALDI−TOF results for the PEO(5000) series are also included in Table 1. Figure 4 is a representative MALDI−TOF spectra for PEO(5k)-1.5G. These results are very similar to those of the Frechet group for benzyl ether dendrimer based hybrid diblocks, [14]8c. MALDI−TOF results agree well with theoretically expected molecular weight for the diblocks as shown in Table 1, suggesting the presence of very few defects in the final structure. Polydispersities calculated from the MALDI−TOF spectra are about 1.01. For the PEO(2000)-dendrimer diblock series, the MALDI−TOF results are available only for PEO(2k)-3.0G. Here too, the measured molecular weight is very close to the theoretically expected value (see Appendix). Though qualitative, FTIR spectra confirm the results obtained from $^1H$ NMR. The peak positions, as reported in the Experimental Section and Appendix, are in good agreement with previous values obtained by other researchers for a similar class of materials.[9,15]

**3.2. Thermal Characterization.** The thermal behavior of the PEO(5000)-dendrimer diblock series was investigated using differential scanning calorimetry (DSC). Figure 5a shows the melting point of the PEO block plotted against the generation number of the dendrimer block. The melting point of the PEO block decreases with increase in the size of the dendrimer block. Pure PEO(5000) had a melting point of 59.5 °C which decreased to 50 °C for the PEO(5000)-4.5G diblock. In Figure 5b, the enthalpy of melting, $\Delta H$ (J/g), is plotted against the generation number of the dendrimer block. The dark squares are the numbers obtained from DSC. The crosses represent the $\Delta H$ values normalized against the weight fraction of PEO in the diblock copolymer. The normalized $\Delta H$ values remain nearly constant with increasing generation number (Figure 5b), implying a constant percentage of crystallinity in the PEO block, despite the presence of the dendrimer block.

Frechet et al. have studied the thermal behavior of AB and ABA diblock and triblock copolymers with PEO as the A block and benzyl ether dendrimer as the B block.[16] They found that when the dendrimer block was the majority block, phase mixing took place with no detectable melting point for the PEO block in the DSC trace due to loss of crystallinity in the mixed phase. When the mass of the PEO block was greater than or equal to the benzyl ether dendrimer block, microphase segregation was found to occur with two thermal transitions being observed—a melting transition associated

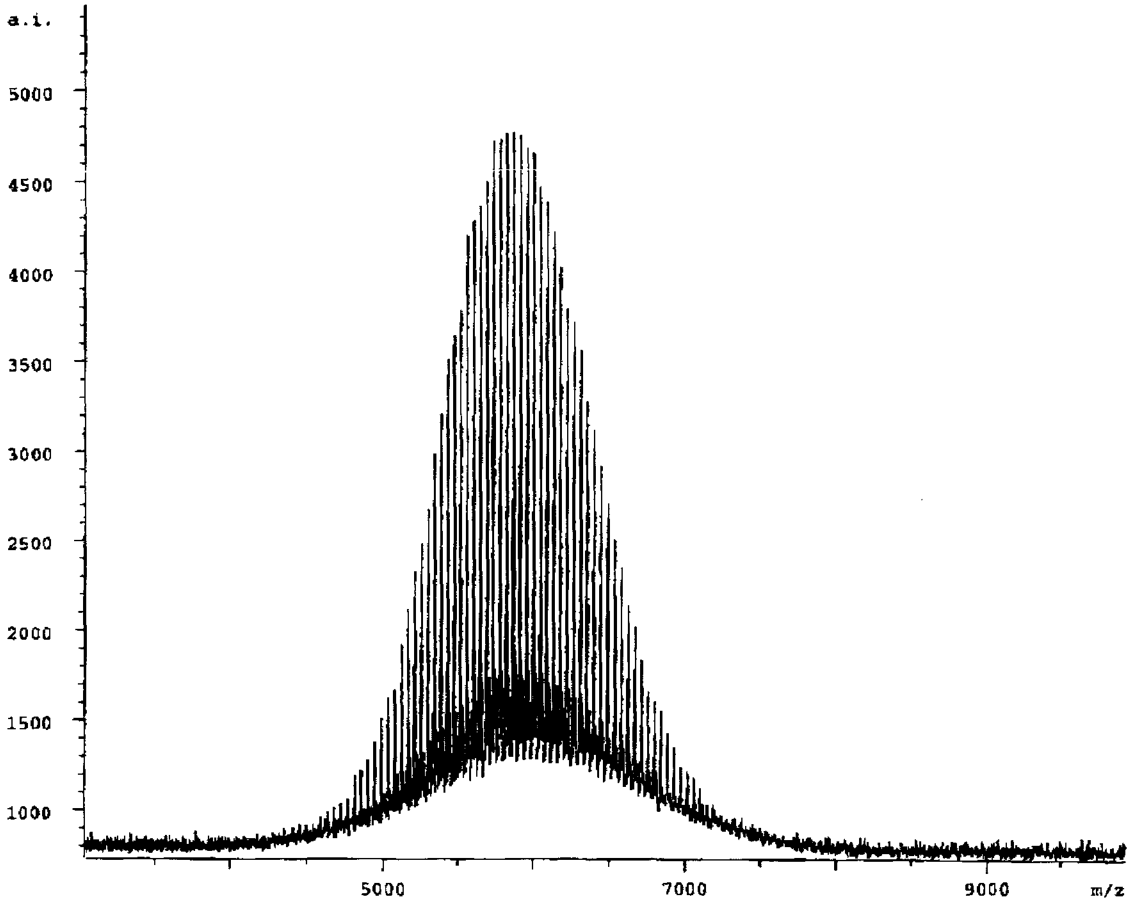

**Figure 4.** MALDI–TOF spectra of PEO(5000)-1.5G.

with the crystalline PEO phase and a glass transition associated with the dendrimer phase.

For the PEO(5000)–PAMAM dendrimer diblocks discussed here, the mass of the PEO block is in excess of the dendrimer for all samples except for PEO(5000)-4.5G, and a melting point for the PEO block is detected in all cases. These results (Figure 5a,b) suggest that the crystalline morphology of the PEO block changes as the dendrimer generation increases, perhaps due to differences in crystallite sizes due to varying block copolymer domain sizes or geometries, or the lowering of $T_m$ due to an increased extent of mixing with larger dendron blocks. However, the constant percent crystallinity strongly suggests that some degree of microphase segregation is present in all cases although further studies are needed to elucidate a more complete picture of the bulk morphology.

Glass transition temperatures ($T_g$) were observed for PEO(5000)-3.0G,3.5G,4.0G,4.5G diblocks, and the presence of end group influence on $T_g$ in linear-dendritic hybrid diblock copolymers is reported here. Figure 6 shows the glass transition temperatures plotted against the generation number of the dendrimer. These glass transition temperatures depend on the chemical nature of the dendrimer end groups with a 30 °C difference between the amine terminated (3.0G, 4.0G) and the ester terminated (3.5G, 4.5G) diblocks. (The $T_g$ of pure PEO(5000) was close to the lower detection limits of the instrument and was not observable.) The strong dependence on end group functionality indicates that the PAMAM dendritic block is the source of the observed $T_g$. This end group effect on $T_g$ has been seen before in pure dendrimers,[17] although this is the first report of such behavior in linear-dendritic hybrid copolymers. For benzyl ether dendrimers, increases in $T_g$'s follow increases in chain end polarities. Literature values of $T_g$'s for pure PAMAM dendrimers are not available for comparison.

**3.3. Solution Behavior. PEO(2000)-Dendrimer Series.** Figure 7a is a graph of the intrinsic viscosity of the PEO(2000)-dendrimer series in unbuffered MilliQ water plotted against the generation number of the dendrimer block. As expected, the addition of the dendritic block changes the $[\eta]$ by small but measurable amounts with a trend of increasing $[\eta]$ with increasing generation number. The Mark–Houwink–Sakurada plot to obtain the **K** and **a** values for this system is shown in Figure 7b. A reasonably good linear relationship is obtained with the **K** and **a** values being 0.414 mL/g and 0.386, respectively. The **K** values obtained from literature for PEO(2000)[18] and PAMAM dendrimer[15] are 0.67 mL/g and 0.776 mL/g respectively; the corresponding **a** values are 0.28 and 0.237. These **a** values obtained from literature for PEO(2000) and PAMAM dendrimer are both a little lower than those for classic linear polymers which are usually in the range of 0.5 to 0.8. The lower value of **a** (0.237) in the case of the PAMAM dendrimer compares favorably with the soft spheroidal structures these polymers are expected to possess and also their symmetrically branched architecture. The value of 0.28 for linear PEO in water at 30 °C is applicable only in the low molecular weight range and it is conjectured that the short PEO chains cannot be treated as semipermeable coils. In comparison, the measured value of 0.386 for the PEO(2000)–PAMAM diblock copolymer is a little higher and sug-

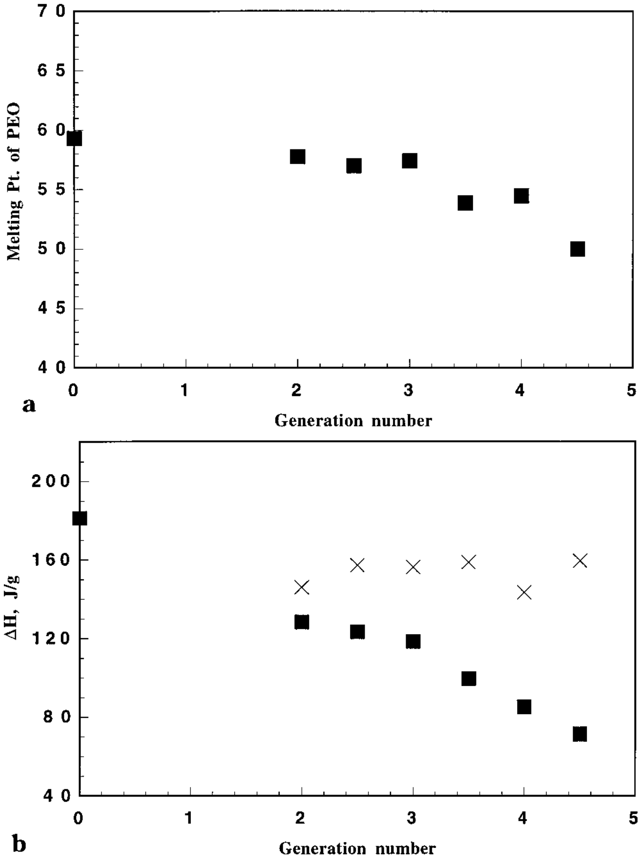

**Figure 5.** (a) Depression of PEO melting point with increasing dendrimer generations in PEO(5000)-dendrimer diblocks. (b) Enthalpy change for PEO melting as a function of dendrimer generation: (■) Δ*H* J/g from DSC; (×) normalized Δ*H* J/g.

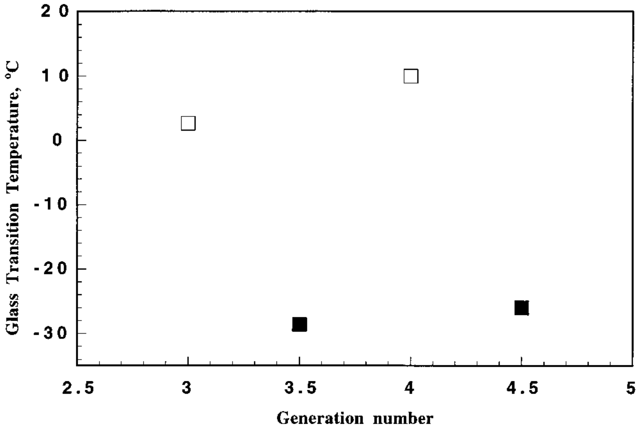

**Figure 6.** Plot of observed glass transition temperature vs dendrimer generation for PEO(5000)-dendrimer diblocks. (□) amine terminal groups, (■) ester terminal groups.

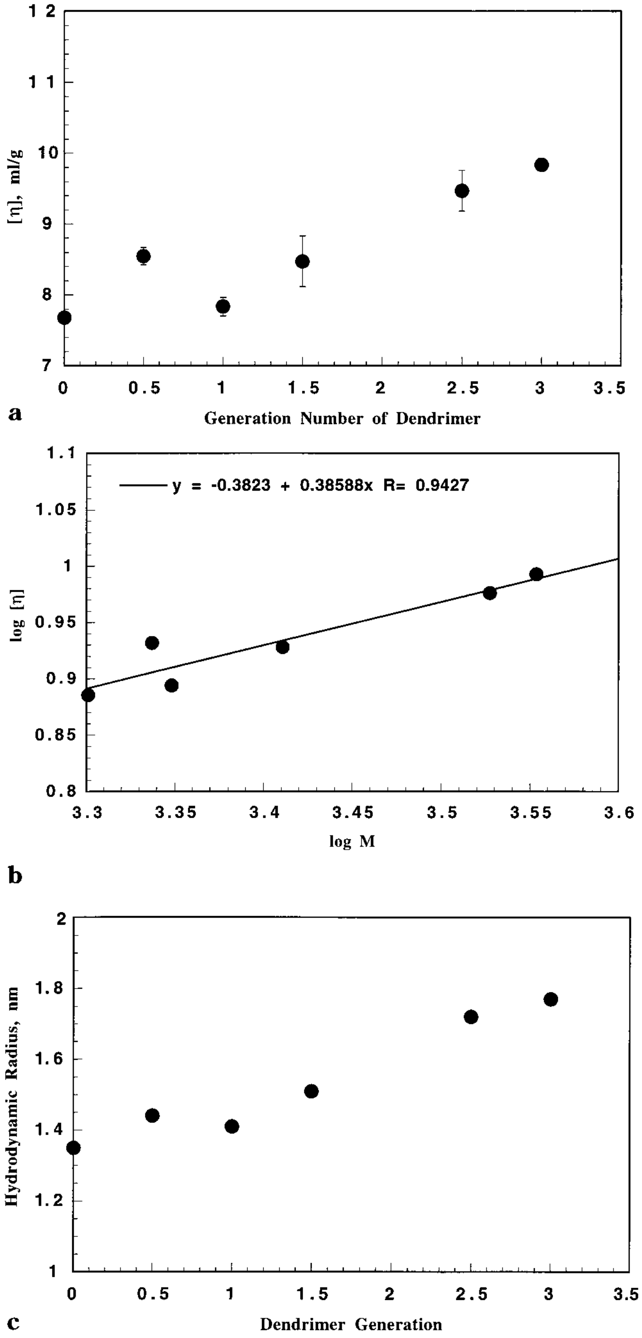

**Figure 7.** (a) Variation of intrinsic viscosity with dendrimer generation for PEO(2000)-dendrimer diblock at 30 °C in water. (b) Relation between intrinsic viscosity and molecular weight for PEO(2000)-dendrimer diblocks. (c) Plot of hydrodynamic radius vs dendrimer generation for PEO(2000)-dendrimer diblocks.

gests that the diblock copolymer is slightly more expanded than its component homopolymers.

Using the Einstein equivalent sphere model equation relating the $[\eta]$ to the hydrodynamic volume and molecular weight, and assuming a spherical shape for the diblock, a hydrodynamic radius, $r_h$, can be calculated. A plot of the calculated $r_h$ vs the generation number of the dendrimer is shown in Figure 7c. $r_h$ increases with increasing generation number as well.

**PEO(5000)-Dendrimer Series.** The relationship between $[\eta]$ in water and the generation number of the dendrimer for the PEO(5000)-dendrimer diblock series is very different from that of the PEO(2000) series. Figure 8a is a plot of $[\eta]$ vs the generation number for the PEO(5000)-half generation diblocks, and Figure 8b is a corresponding plot for the PEO(5000)-full generation diblocks. For all of the copolymers with the exception of PEO(5000)-4.0G, $[\eta]$ is lower than that for the linear PEO(5000) core. This behavior may be explained by the formation of a PEO corona shielding the hydrophobic dendrimer repeat unit from the solvent, which results in a decrease in $[\eta]$. This decrease for early generations of other linear-dendritic diblock series due to the formation of unimolecular micellar structures was observed earlier by Gitsov and Frechet.[19] They found that for PEO(7500)−benzyl ether dendrimers, the attachment

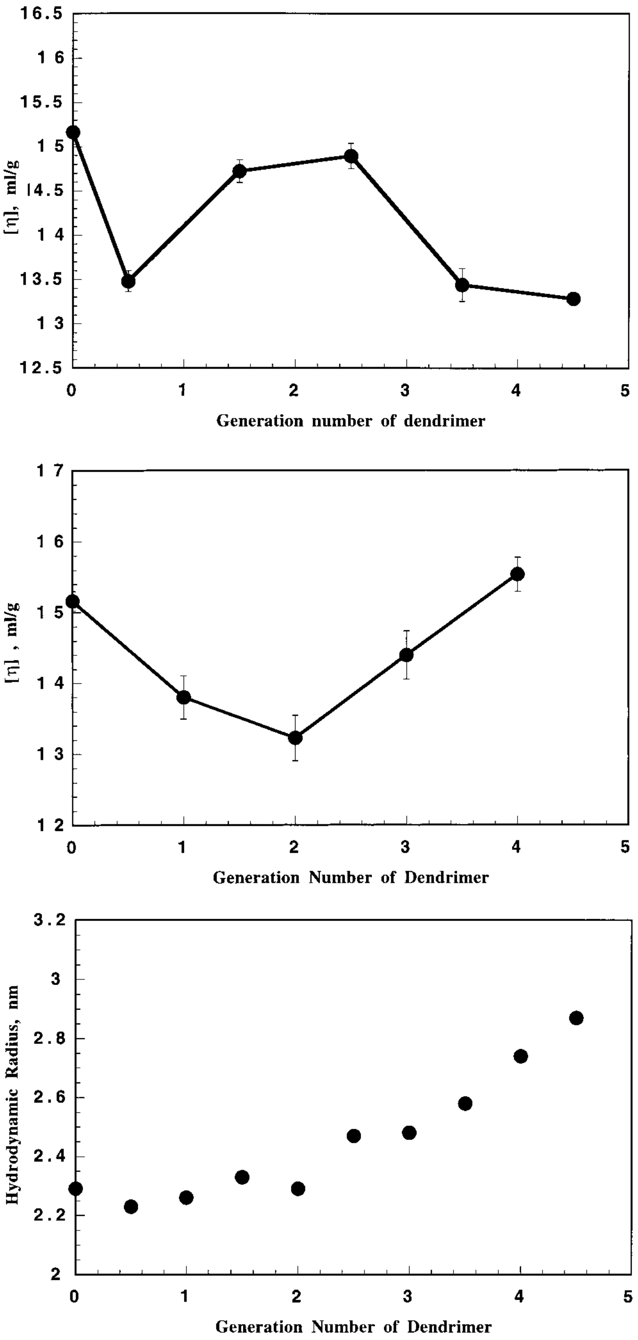

**Figure 8.** (a) Variation of intrinsic viscosity with dendrimer half generation for PEO(5000)-dendrimer diblocks at 30 °C in water. (b) Variation of intrinsic viscosity with dendrimer full generation for PEO(5000)-dendrimer diblocks at 30 °C in water. (c) Variation of hydrodynamic radius with generation number for PEO(5000)-dendrimer diblocks.

of the first generation to the linear PEO notably decreased the intrinsic viscosity in THF.

In the case of full generation PEO(5000)-dendrimer diblocks (Figure 8b), favorable interaction of the PEO with the amine end groups probably furthers collapse of the PEO chain initially. The favorable interactions cannot compensate for the increasing size of the dendron with increasing generation number. Increase in generation number is accompanied by an exponential increase in the number of hydrophilic amine groups. As the number of amine groups increases, the hydrophilicity of the dendrimer block increases, and PEO no longer needs to shield the dendrimer and may be too short to do so.

The intrinsic viscosity curve obtained for the PEO(5000)-dendrimer with ester end groups indicates that the ester functionality results in very different solution behavior. The trend includes a maximum in $[\eta]$ with increasing generation number which mirrors the trends observed for traditional spherical dendrimers.[1,20] For pure PAMAM and benzyl ether dendrimers, the intrinsic viscosity goes through a maximum at a given generation of the dendrimer. In this case, methyl ester may be water compatible at low generation numbers due to the presence of amide groups and ester polarity. However, PEO/methyl ester interactions may be less favorable than PEO/$NH_2$ interactions, and less shielding takes place initially. As the dendrimer gets bigger, the relative increase in molecular weight is greater than the increase in molecular size; as a result, the intrinsic viscosity, which is a ratio of size with molecular weight, decreases as observed in dendrimer homopolymers.

The unimolecular micelle or shielding effect is seen in the PEO(5000)-dendrimer series, but not in the PEO(2000)-dendrimer series, due to the increased chain length of the PEO block. For example, although the weight fractions of the two blocks in both PEO(2000)-3.5G and PEO(5000)-4.5G are approximately the same, the size ratio of the PEO block to the dendrimer block is larger for the PEO(5000) diblock. Using hydrodynamic radii from intrinsic viscosity measurements, the size ratio of the PEO(2000) homopolymer to dendrimer homopolymer(3.5G)[15] is 13 Å:12.9 Å, whereas the size ratio of PEO(5000) to dendrimer homopolymer(4.5G)[15] is 23 Å:16.8 Å. This dependence of the shielding effect on linear chain length has been observed by other researchers.[19] ABA triblock copolymers where the A block is dendritic and the B block is linear also show this behavior.[21] What is interesting with respect to the polymers described here is the relatively low molecular weight of PEO at which the shielding behavior is observed; in earlier studies, shielding effects were observed for linear PEO block molecular weights of 7500−26000.

The differing intrinsic viscosity behavior between the PEO(2000) and PEO(5000) diblock series may also be influenced by the behavior of the PEO homopolymer in water. Literature results show a transition in the Mark−Houwink parameters (**K** and **a**) for PEO linear polymers at an approximate molecular weight of 3000.[18] Below this molecular weight, the **a** value is low, suggesting a less expanded polymer conformation; however, above this molecular weight the **a** value is 0.78, suggesting a highly expanded polymer in a good solvent. This is probably another factor that should be accounted for in analyzing the different shielding behavior exhibited by the diblock copolymers.

Converting the $[\eta]$ to hydrodynamic radii, $r_h$, using the Einstein equivalent sphere model mentioned earlier, gives a more direct picture of what happens in aqueous solutions of PEO(5000)-dendrimer diblocks. The graph of $r_h$ plotted against dendrimer generation is shown in Figure 8c. The hydrodynamic radius exhibits a decrease due to the previously described shielding effects until the second generation, and then increases with increasing generation number.

**GPC Results.** Two other techniques, GPC and dynamic light scattering, were used to further probe the solution behavior of the synthesized diblocks and to corroborate the behavior seen in the intrinsic viscosity experiments. Average GPC values for the molecular

**Table 2. GPC Results for PEO−PAMAM Diblock Copolymers**

| material | hydrodynamic radius, nm |
|---|---|
| PEO(5000)−0.5G | 2.27 |
| PEO(5000)−1.0G | 1.61 |
| PEO(5000)−1.5G | 2.06 |
| PEO(5000)−2.0G | |
| PEO(5000)−2.5G | 2.11 |
| PEO(5000)−3.0G | 2.16 |
| PEO(5000)−3.5G | 2.27 |
| PEO(5000)−4.0G | 2.27 |
| PEO(5000)−4.5G | 2.16 |
| PEO(2000)−0.5G | 1.26 |
| PEO(2000)−1.0G | |
| PEO(2000)−1.5G | 1.13 |
| PEO(2000)−2.0G | 1.34 |
| PEO(2000)−2.5G | |
| PEO(2000)−3.0G | 1.38 |

weight of the PEO(2000)-dendrimer diblocks were ∼2200 and those for the PEO(5000)-dendrimer diblocks were ∼6000. Use of the calibration curve based on linear poly(ethylene oxide) standards did not give good overall estimates of the molecular weight. These observations suggest a deviation from the behavior of linear polymers consistent with the intrinsic viscosity results. There are two factors in the GPC experiments that could further modulate the effects and, hence, prevent the exhibition of trends seen in the intrinsic viscosity experiments: (a) the buffered aqueous mobile phase, which may have reduced the influence of the dendrimer end group functionality on the size and shape of the diblock for the PEO(5000) series, and (b) the existence of secondary interactions of the dendrimer block with the column packing. The PEO(2000)-dendrimer diblocks are probably too close to the size of the lowest molecular weight standard to show specific trends in GPC. The hydrodynamic volume from the GPC results were converted to an equivalent hydrodynamic radius using the Einstein equivalent sphere model equation (see Table 2). The hydrodynamic radii from the two techniques fall in the same range but the clear trend seen in the intrinsic viscosity measurements is not apparent in the GPC results. Dynamic light scattering experiments were done in MilliQ water at 30 °C for some of the PEO(5000) diblocks. The PEO(2000) diblocks were too small to be studied with the dynamic light scattering setup used. The values for copolymer size obtained from dynamic light scattering techniques also fall in the same range as those calculated from intrinsic viscosity and GPC measurements. However, intrinsic viscosity remains the most sensitive and reliable technique for determining the hydrodynamic size of these materials.

## 4.0. Summary and Conclusions

A series of new linear-dendrimeric block copolymers have been synthesized in which the linear block is PEO and the dendrimeric block is PAMAM. Thermal characterization suggests that these diblock copolymers exhibit some degree of microphase segregation irrespective of the composition of the diblock. Glass transition temperatures were observed for some of the diblocks. Dependence of glass transition on end group functionality of the dendrimer block was observed for the first time in such linear-dendrimeric hybrid copolymers. Intrinsic viscosity studies show that the solution behavior is greatly affected by the length of the PEO linear chain at low molecular weights, and the number and chemical nature of the dendrimer end group. PEO(2000)-dendrimer diblocks exhibit increasing $[\eta]$ with increasing molecular weight as is observed for traditional linear polymers. For the PEO(5000)-dendrimer diblocks, $[\eta]$ decreases with the introduction of the dendrimer block, suggesting a unimicellar like structure formed by wrapping of the PEO chain around the dendrimer block. The variation of $[\eta]$ with dendrimer generation in the PEO(5000) series is reminiscent of the relationship seen for pure dendrimers. Further investigation into the properties of these diblock copolymers is underway, particularly as ultrathin films, and will be described in a forthcoming publication.

**Acknowledgment.** Financial support for this work came from the Environmental Protection Agency (Grant No. R825224-01-0). The authors would like to thank Leticia Cornett of Bruker-Daltonics Analytical Systems for doing the MALDI−TOF MS measurements reported in this paper.

## Appendix

**PEO(2000)-0.5G.** $^1$H NMR in DMSO-$d_6$: $\delta_{\mathrm{PEO}}(\mathrm{C}\mathbf{H}_2\mathrm{C}\mathbf{H}_2\mathrm{O})$ = 3.511 (b); $\delta_{\mathrm{PEO}}(\mathrm{C}\mathbf{H}_3\mathrm{O}-)$ = 3.242 (s); $\delta_{\mathrm{PAMAM}}(-\mathrm{COOC}\mathbf{H}_3)$ = 3.574 (s); $\delta_{\mathrm{PAMAM}}(-\mathrm{C}\mathbf{H}_2\mathrm{COOCH}_3)$ = 2.396 (t); $\delta_{\mathrm{PAMAM}}$(protons next to tertiary amines) = 2.55−2.8. FTIR, $\nu$ cm$^{-1}$: 1114, 1736, 2883.

**PEO(2000)-1.0G.** $^1$H NMR in D$_2$O: $\delta_{\mathrm{PEO}}(\mathrm{C}\mathbf{H}_2\mathrm{C}\mathbf{H}_2\mathrm{O})$ = 3.612 (b); $\delta_{\mathrm{PEO}}(\mathrm{C}\mathbf{H}_3\mathrm{O}-)$ = 3.290 (s); $\delta_{\mathrm{PAMAM}}(-\mathrm{C}\mathbf{H}_2\text{-}\mathrm{CONH}-)$ = 2.355 (t); $\delta_{\mathrm{PAMAM}}(-\mathrm{CONHC}\mathbf{H}_2-)$ = 3.185 (t); $\delta_{\mathrm{PAMAM}}$(protons next to primary and tertiary amines) = 2.6−2.8. FTIR, $\nu$ cm$^{-1}$: 1115, 1547, 1657, 2880, 3243.

**PEO(2000)-1.5G.** $^1$H NMR in DMSO-$d_6$: $\delta_{\mathrm{PEO}}(\mathrm{C}\mathbf{H}_2\mathrm{C}\mathbf{H}_2\mathrm{O})$ = 3.511 (b); $\delta_{\mathrm{PEO}}(\mathrm{C}\mathbf{H}_3\mathrm{O}-)$ = 3.243 (s); $\delta_{\mathrm{PAMAM}}(-\mathrm{COOC}\mathbf{H}_3)$ = 3.581 (s); $\delta_{\mathrm{PAMAM}}(-\mathrm{C}\mathbf{H}_2\mathrm{CONH}-)$ = 2.16 (m); $\delta_{\mathrm{PAMAM}}(-\mathrm{CONHC}\mathbf{H}_2-)$ = 3.046 (m); $\delta_{\mathrm{PAMAM}}$-$(-\mathrm{C}\mathbf{H}_2\mathrm{COOCH}_3)$ = 2.398 (t); $\delta_{\mathrm{PAMAM}}$(protons next to tertiary amines) = 2.5−2.8. FTIR, $\nu$ cm$^{-1}$: 1112, 1539, 1661, 1734, 2875, 3248.

**PEO(2000)-2.0G.** $^1$H NMR in D$_2$O: $\delta_{\mathrm{PEO}}(\mathrm{C}\mathbf{H}_2\mathrm{C}\mathbf{H}_2\mathrm{O})$ = 3.619 (b); $\delta_{\mathrm{PEO}}(\mathrm{C}\mathbf{H}_3\mathrm{O}-)$ = 3.296 (s); $\delta_{\mathrm{PAMAM}}(-\mathrm{C}\mathbf{H}_2\text{-}\mathrm{CONH}-)$ = 2.353 (m); $\delta_{\mathrm{PAMAM}}(-\mathrm{CONHC}\mathbf{H}_2-)$ = 3.19 (m); $\delta_{\mathrm{PAMAM}}$(protons next to primary and tertiary amines) = 2.5−2.8. FTIR, $\nu$ cm$^{-1}$: 1113, 1541, 1657, 2875, 3243.

**PEO(2000)-2.5G.** $^1$H NMR in DMSO-$d_6$: $\delta_{\mathrm{PEO}}(\mathrm{C}\mathbf{H}_2\mathrm{C}\mathbf{H}_2\mathrm{O})$ = 3.511 (b); $\delta_{\mathrm{PEO}}(\mathrm{C}\mathbf{H}_3\mathrm{O}-)$ = 3.241 (s); $\delta_{\mathrm{PAMAM}}(-\mathrm{COOC}\mathbf{H}_3)$ = 3.577 (s); $\delta_{\mathrm{PAMAM}}(-\mathrm{C}\mathbf{H}_2\mathrm{CONH}-)$ = 2.178 (m); $\delta_{\mathrm{PAMAM}}(-\mathrm{CONHC}\mathbf{H}_2-)$ = 3.06 (m); $\delta_{\mathrm{PAMAM}}$-$(-\mathrm{C}\mathbf{H}_2\mathrm{COOCH}_3)$ = 2.412 (m); $\delta_{\mathrm{PAMAM}}$(protons next to tertiary amines) = 2.5−2.8. FTIR, $\nu$ cm$^{-1}$: 1104, 1541, 1662, 1733, 2864, 3232.

**PEO(2000)-3.0G.** $^1$H NMR in D$_2$O: $\delta_{\mathrm{PEO}}(\mathrm{C}\mathbf{H}_2\mathrm{C}\mathbf{H}_2\mathrm{O})$ = 3.60 (b); $\delta_{\mathrm{PEO}}(\mathrm{C}\mathbf{H}_3\mathrm{O}-)$ = 3.28 (s); $\delta_{\mathrm{PAMAM}}(-\mathrm{C}\mathbf{H}_2\text{-}\mathrm{CONH}-)$ = 2.33 (m); $\delta_{\mathrm{PAMAM}}(-\mathrm{CONHC}\mathbf{H}_2-)$ = 3.17 (m); $\delta_{\mathrm{PAMAM}}$(protons next to primary and tertiary amines) = 2.5−2.8. FTIR, $\nu$ cm$^{-1}$: 1107, 1546, 1658, 2870, 3254. $M_{\mathrm{w}}$(theoretical) = 3576; $M_{\mathrm{w}}$(MALDI−TOF) = 3450.

**PEO(2000)-3.5G.** $^1$H NMR in CDCl$_3$: $\delta_{\mathrm{PEO}}(\mathrm{C}\mathbf{H}_2\mathrm{C}\mathbf{H}_2\mathrm{O})$ = 3.663 (b); $\delta_{\mathrm{PEO}}(\mathrm{C}\mathbf{H}_3\mathrm{O}-)$ = 3.4 (s); $\delta_{\mathrm{PAMAM}}(-\mathrm{COOC}\mathbf{H}_3)$ = 3.688 (s); $\delta_{\mathrm{PAMAM}}(-\mathrm{C}\mathbf{H}_2\mathrm{CONH}-)$ = 2.382 (m); $\delta_{\mathrm{PAMAM}}$-$(-\mathrm{CONHC}\mathbf{H}_2-)$ = 3.3 (m); $\delta_{\mathrm{PAMAM}}(-\mathrm{C}\mathbf{H}_2\mathrm{COOCH}_3)$ = 2.453 (m); $\delta_{\mathrm{PAMAM}}$(protons next to tertiary amines) = 2.5−2.9. FTIR, $\nu$ cm$^{-1}$: 1110, 1539, 1662, 1734, 2864, 3243.

**PEO(2000)-4.0G.** $^1$H NMR in D$_2$O: $\delta_{\mathrm{PEO}}(\mathrm{C}\mathbf{H}_2\mathrm{C}\mathbf{H}_2\mathrm{O})$ = 3.574 (b); $\delta_{\mathrm{PEO}}(\mathrm{C}\mathbf{H}_3\mathrm{O}-)$ = 3.252 (s); $\delta_{\mathrm{PAMAM}}(-\mathrm{C}\mathbf{H}_2\text{-}\mathrm{CONH}-)$ = 2.299 (m); $\delta_{\mathrm{PAMAM}}(-\mathrm{CONHC}\mathbf{H}_2-)$ = 3.151

(m); $\delta_{\mathrm{PAMAM}}$(protons next to primary and tertiary amines) = 2.5−2.8. FTIR, $\nu$ cm$^{-1}$: 1109, 1549, 1647, 2864, 2919, 3281.

## References and Notes

(1) Tomalia, D. H.; Naylor, A. M.; Goddard, W. A., III. *Angew. Chem., Int. Ed.* **1990**, *29*, 138−173.

(2) Wooley, K. L.; Hawker, C. J.; Fréchet, J. M. J. *J. Am. Chem. Soc.* **1991**, *113*, 4252−4261.

(3) Newkome, G. R.; Moorefield, C. N.; Vogtle, F. *Dendritic Molecules: Concepts, Syntheses, Perspectives*; VCH Publishers: New York, 1996.

(4) Matthews, O. A.; Shipway, A. N.; Stoddart, J. F. *Prog. Polym. Sci.* **1998**, *23*, 1−56.

(5) Chapman, T. M.; Hillyer, G. L.; Mahan, E. J.; Shaffer, K. A. *J. Am. Chem. Soc.* **1994**, *116*, 11195.

(6) (a) van Hest, J. C. M.; Delnoye, D. A. P.; Baars, M. W. P. L.; van Genderen, M. H. P.; Meijer, E. W. *Science* **1995**, *268*, 1592. (b) van Hest, J. C. M.; Baars, M. W. P. L.; Elissen-Román, C.; van Genderen, M. H. P.; Meijer, E. W. *Macromolecules* **1995**, *28*, 6689.

(7) (a) Gitsov, I.; Wooley, K. L.; Hawker, C. J.; Ivanova, P. T.; Fréchet, J. M. J. *Macromolecules* **1993**, *26*, 5621−5627. (b) Gitsov, I.; Frechet, J. M. J. *Macromolecules* **1994**, *27*, 7309−7315.

(8) (a) Matyjaszewski, K.; Shigemoto, T.; Fréchet, J. M. J.; Leduc, M. *Macromolecules* **1996**, *29*, 4167. (b) Leduc, M.; Hawker, C. J.; Dao, J.; Fréchet, J. M. J. *J. Am. Chem. Soc.* **1996**, *118*, 11111. (c) Leduc, M. R.; Hayes, W.; Fréchet, J. M. J. *J. Polym. Sci. Polym. Chem.* **1998**, *36*, 1.

(9) Aoi, K.; Motoda, A.; Okada, M. *Macromol. Rapid. Commun.* **1997**, *18*, 945−952.

(10) Fréchet, J. M. J.; Gitsov, I. *Macromol. Symp.* **1995**, *98*, 441.

(11) Hîgberg, T.; Ström, P.; Ebner, M.; Rämsby, S. *J. Org. Chem.* **1987**, *52*, 2033.

(12) Iyer, J.; Hammond, P. T. *Langmuir*, in press.

(13) (a) Tomalia, D. A.; Dewald, J. R. U.S. Patent 4 568 737, Feb 4, 1986. (b) Tomalia, D. A.; Baker, H.; Dewald, J.; Hall, M.; Kallos, G.; Roeck, J.; Ryder, J.; Smith, P. *Macromolecules* **1986**, *19*, 2466.

(14) Leon, J. W.; Fréchet, J. M. J. *Polym. Bull.* **1995**, *35*, 449.

(15) Tomalia, D. A.; Baker, H.; Dewald, J.; Hall, M.; Kallos, G.; Martin, S.; Roeck, J.; Ryder, J.; Smith, P. *Polym. J.* **1985**, *17*, 117−132.

(16) Gitsov, I.; Wooley, K. L.; Hawker, C. J.; Ivanova, P. T.; Fréchet, J. M. J. *Macromolecules* **1993**, *26*, 5621−5627.

(17) Wooley, K. L.; Hawker, C. J.; Pochan, J. M.; Fréchet, J. M. J. *Macromolecules* **1993**, *26*, 1514−1519.

(18) Bailey, F. E., Jr.; Koleske, J.V. *Poly(ethylene oxide)*; Academic Press: New York, 1976.

(19) Gitsov, I.; Fréchet, J.M. J. *Macromolecules* **1993**, *26*, 6536−6546.

(20) Mourey, T. H.; Turner, S. R.; Rubinstein, M.; Fréchet, J. M. J.; Hawker, C. J.; Wooley, K. L. *Macromolecules* **1992**, *25*, 2401−2406.

(21) Gitsov, I.; Fréchet, J. M. J. *Macromolecules* **1994**, *27*, 7309−7315.

MA980654G